ARAŞTIRMA MAKALESİ / RESEARCH ARTICLE

MODELING AND SIMULATION TO INVESTIGATE THE THERMAL EFFICIENCY OF A PARABOLIC SOLAR TROUGH COLLECTOR WITH ABSORBER TUBE INSERTED TWISTED TAPE SYSTEM

Mohammed Faris ABBAS[1]
[1]School of Engineering and Natural Sciences, Altinbas University, Istanbul, Turkey
mohammed89_eng@yahoo.com ORCID No: 0000-0002-8034-0376

İbrahim KOÇ[2]
[2]School of Engineering and Natural Sciences, Altinbas University, Istanbul, Turkey
ibrahim.koc@altinbas.edu.tr ORCID No: 0000-0002-1379-7093

Ahmed F. Khudheyer ALJANABI[3]
[3]Mechanical Engineering Department, Al-Nahrain University, Baghdad, Iraq
drahmed955@eng.nahrainuniv.edu.iq ORCID No: 0000-0002-5809-4105

Abstract

Concentrated solar power is one of the renewable energy sources in the world that can be utilized from solar energy by combining and concentrating it. In this numerical study, computer software was used to investigate the parabolic trough collector consists of a mirror and tube made of copper covered with a vacuum glass. The twisted tape made of aluminum is placed inside the tube to generate swirl flow and turbulence around the axial centerline of the absorber tube with the working fluid. Water was used as a working fluid with turbulent flow, the Reynolds number varied for the range of 2000 to 9000. To describe the present study, continuity, momentum, and energy equations were used. The angle of inclination of the twisted tape has been taken into account in six different values: 25 °, 33 °, 45 °, 50 °, 55 °, and 60 °. A study occurred in the city of Istanbul in Turkey with 41° latitude and 28.97° longitude for a periodic time from 9:00 am to 3:00 pm, for four different selected months, September, October, November, and December. Results illustrated increasing in outlet temperature and heat transfer enhancement for six twisted tape angles compared with the plain tube. The best angle of inclination of the twisted tape was found to be 50 degrees.

Keywords: Concentrating solar power, Parabolic trough collector, Twisted tape, Heat transfer enhancement.

EMİCİ TÜP İÇİNE BÜKÜMLÜ BANT YERLEŞTİRİLMİŞ BİR PARABOLİK OLUKLU GÜNEŞ KOLLEKTÖRÜNÜN ISIL VERİMİNİ ARAŞTIRMAK İÇİN MODELLEME VE SİMÜLASYON

Özet

Yoğunlaştırılmış güneş enerjisi, güneş enerjisinin birleştirilmesi ve yoğunlaştırılarak kullanılabilen dünyadaki yenilenebilir enerji kaynaklarından biridir. Bu sayısal çalışmada, bir ayna ve vakumlu camla kaplı bakırdan yapılmış tüpten oluşan parabolik oluklu kolektörün incelenmesi için bilgisayar yazılımı kullanılmıştır. Alüminyumdan yapılmış bükülmüş bant, çalışma sıvısı ile emici tüpün eksenel merkez hattı etrafında girdap akışı ve türbülans oluşturmak için tüpün içine yerleştirilmiştir. Su, Reynolds sayısı 2000 ile 9000

arasında değişen türbülans akışlı bir çalışma sıvısı olarak kullanılmıştır. Bu çalışmayı tanımlamak için süreklilik, momentum ve enerji denklemleri kullanılmıştır. Bükümlü bandın eğim açısı 25 °, 33 °, 45 °, 50 °, 55 ° ve 60 ° olmak üzere altı farklı değerde dikkate alınmıştır. Türkiye'nin İstanbul şehrinde 41 ° enlem ve 28.97 ° boylamda, Eylül, Ekim, Kasım ve Aralık olmak üzere seçilen dört farklı ay için 09:00 - 15:00 arasında periyodik bir süre için bir çalışma gerçekleştirilmiştir. Sonuçlar, düz boru ile karşılaştırıldığında altı bükümlü bant açısı için çıkış sıcaklığındaki ve ısı transferindeki artışın olduğunu göstermektedir. Bükümlü bandın en iyi eğim açısı 50 derece olarak bulunmuştur.

Anahtar Kelimeler: Konsantre güneş enerjisi sistemleri, Parabolik oluklu kolektör, bükülmüş bant, Isı transferini iyileştirme

1. INTRODUCTION

Interest in renewable energy sources increases recently. The most suitable energy source for specific regions in the world is obviously solar energy because of its many uses, including the conversion of solar energy into electrical energy through panels or into thermal energy. And to take advantage of the converted solar energy into thermal through the technology of collecting this energy by the parabolic trough collector (PTC), dish system, and power tower or central receiving system (CRS) (Padilla 2011).

PTC is one of the most used applications in solar energy, which consists of a mirror that reflects the sun rays falling on it and focuses it on the absorber tube in order to heat the working fluid.

To enhancement the heat transfer inside the tube, there are two techniques, the active method, and the passive method. Active methods requiring external power, passive methods do not require any additional power and are performed by changing a geometry design. The twisted tape is one of the passive methods to enhance heat transfer by generate swirl flow and make a mixing between the fluid near the surface with the center of the tube. The collector in figure 1, was used in this study has a 1220 mm length of the mirror and 1668 mm width with reflectivity 0.9, The tube was made from a capper with 23 mm inner diameter and 25 mm outer diameter with absorptivity of 0.95 and covered by glass with transmissivity 0.85. This tube exposed to heat that reflected from the collector with a concentration ratio of 20.598, the upper surface area directly from the sun and the lower surface area from reflected rays by the collector, the amount of the limits of the lower area knows by rim angle (ϕ_R), The twisted tape inserts in the tube with a 4.787 twist ratio and 1.2 mm thickness made from aluminum (Bhakta, Panday, and Singh 2018).
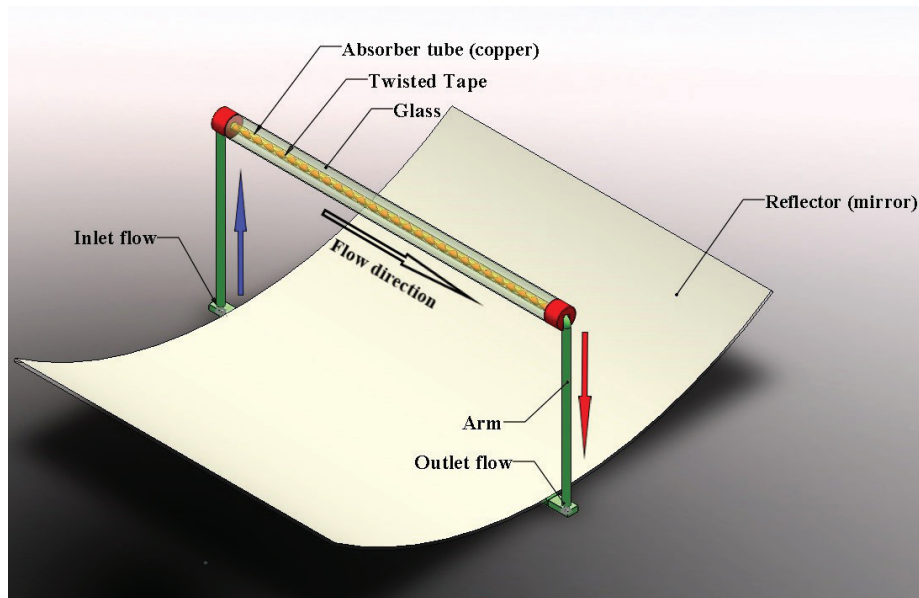
Figure 1. Schematic of parabolic trough collector

In this study, the change of the angle of the twisted tap was numerically investigated for six angles of 25°, 33°, 45°, 50°, 55°, and 60°. The governing equations are solved by using the finite volume method (FVM) by ANSYS FLUENT 2020 R2 software. There is a lot of previous research in parabolic trough collector as following :

(Bhakta, Panday, and Singh 2018) studied the thermal performance of cylindrical parabolic concentrating with water flow by using nail twisted tape and pitch ratios 4.787, 6.914, and 9.042. They found the best solar energy collected and stored water at noon with a nail pitch ratio of 4.787.

(Velazquez-lucho and Robles 2016) developed the thermodynamic model framework to improve the heat transfer performance. with experimental study used the twisted tape ratio of approximately 1 to generate swirl flow with a low Reynolds number.

(Sharma and Kundan 2014) an attempt had been made to enhancement the performance of solar collector through utilized nanofluid instead of water as working fluid they used nanoparticles alumina oxide (Al_2O_3) and copper oxide (CuO), The advantage of nanoparticles was small in size so they cannot make any effect on pumps and can absorb the energy. they looked for an improvement in efficiency.

(Ghadirijafarbeigloo, Zamzamian, and Yaghoubi 2014) discussed the improvement of parabolic trough collector by used new technology louvered twisted tape with a fin. In this numerical simulation study with a deferent twisted ratio of 2.67, 4, and 5.33 they found an increase in Nusselt number and friction factor.

(Yaningsih and Wijayanta 2018) investigated experimentally used twisted tape with three types of wings triangle (T-Tri), rectangle (T-Rec), and trapezoid (T-Tra), twisted ratio 3.8 with the angle of attack at 60° they found the heat transfer and friction factor were enhanced when used wing twisted tape was trapezoid twisted tape because of making the flow more turbulence near the wall of the tube.

(Saravanan et al. 2019) tried to improve the heat transfer in this experimental study by the impact of helically twisted tape ratio (3, 4, 5, and 6), and Reynolds number between 3000 to 23000. They found the **V** trough solar collector with twisted tape improved the heat transfer 8.4% compared with a plain tube and the lower twist ratio (3) gives the best result because of the generated strong swirl and higher hydraulic length.

Feizabadi (Khoshvaght-Aliabadi and Feizabadi 2020) studied numerically to research tubular heat exchangers using a combination of two twisted tape methods. In this method, the twisted tube put inside it twisted tape elliptical cross-section area. The twisted tube installed inside it twisted tape on the minor axis and the twisted tube installed inside it twisted tape on the major axis all compared with straight tube and a straight tube put inside it twisted tape. The higher hydrothermal performance was found in minor more than major at Reynolds number 1800.

(He et al. 2020) explained the impact of twisted tape with CuO-water nanofluid as a working fluid for different concentrations volume from 1 to 4 % in a tube. In this study, they used single and two-phase (mixture) twisted tape in the tube. The result found the single twisted tape was closer to two-phase twisted tape, performance efficiency coefficient with one twisted tape in a tube was 2.18 while with two twisted tapes was 2.04.

(Sivakumar et al. 2020) used CFD simulation to enhancement the heat transfer coefficient, heat transfer, friction factor, and Nusselt number by a used triangular and circular cut in twisted tape, Reynolds number range between 5710 to 18300, and twisted tape ratio 5.4 with laminar flow rate. They found increasing heat transfer more by using triangular cut twisted tape compared with plain twisted tape and a circular hole cut twisted and the heat transfer was improved by 1.02 times more by using triangular cut relative to the circular cut twisted tape.

2. PARABOLIC SOLAR COLLECTOR AND TWISTED TAPE PROPERTIES

In this study, heat transfer fluid (HTF) is water, the fluid enters to the tube with turbulent flow, and Reynolds number Re>2300. The twisted tape was made from aluminum, the characteristic geometries for twisted tape length (l), the diameter of twisted tape (w), thickness (t). The absorber tube was made from copper because of having higher thermal conductivity ($k = 385$ W/mK) when compared to aluminum and steel. The outer surface of the absorber was black coated to work like the similar black body ($\varepsilon \approx 1$) to absorb the heat more than the other color body and to increase the thermal efficiency, with absorptivity (0.95), inner diameter absorber tube (D_i), the absorber tube was wrapped by the glass to working as a greenhouse to minimize radiation heat transfer loss from absorber tube with transmissivity (0.85). Twisted tape with twist ratio (y/w) is the ratio between the pitch tape (y) to the diameter of tape (w). PTC was made from an acrylic mirror with reflectivity (0.9), the total area of the parabolic mirror (A_{ref}), with width (W_p), length (L_p). Focal length (l_f) is the length between the reflector and the absorber tube, the rim angle (ϕ_R) is an angle between the vertical axis and line from the focal point to a parabolic service edge. Figure 2 shows the symbols of PTC. All the data in Table 1, of the collector, have been found in reference(Bhakta, Panday, and Singh 2018). Figures 3 and 4 show the parts and dimensions.
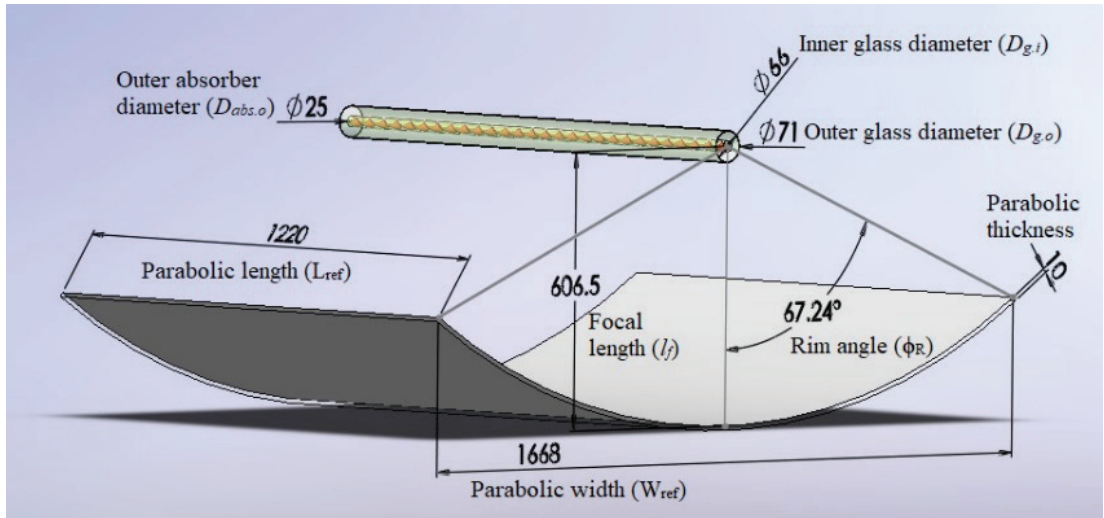
Figure 2. Parabolic trough collector dimensions

Table 1. Dimensions of geometrical parameters (Bhakta, Panday, and Singh 2018)

Parameter	Symbol	Value
Twisted tape length	l	1220 mm
Twisted tape diameter	w	20 mm
Twisted tape thickness	t	1.2 mm
The outer diameter for the absorber tube	$D_{abs.o}$	25 mm
The inner diameter for the absorber tube	$D_{abs.i}$	23 mm
The outer diameter for the glass envelope	$D_{g.o}$	71 mm
The inner diameter for the glass envelope	$D_{g.i}$	66 mm
Twist ratio	y/w	4.787
Pitch tape	y	95.74 mm
Concentration ratio	C	20.598
Area of parabolic trough collector	A	2.036 m^2
Width of the parabolic reflector	W_{ref}	2 x 0.834 m
Length of the parabolic reflector	L_{ref}	1.22 m
Focal length	l_f	606.5 mm
Rim angle	ϕ_R	67.24^0
Absorptivity for an absorber tube	α	0.95
Reflectivity for a parabolic mirror	ρ	0.9
Transmissivity of the glass envelope	τ	0.85
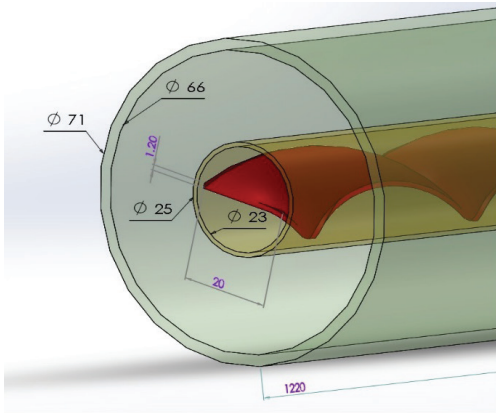
Figure 3. Dimensions of twisted tape, copper, and glass
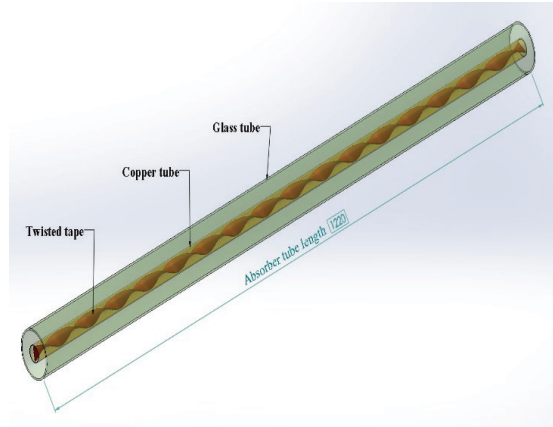
Figure 4. Twisted tape covered by copper and glass tube

In this study, there are six different twisted tape angles 25°, 33°, 45°, 50°, 55°, and 60°. In Figure 5 shown 3 angles:
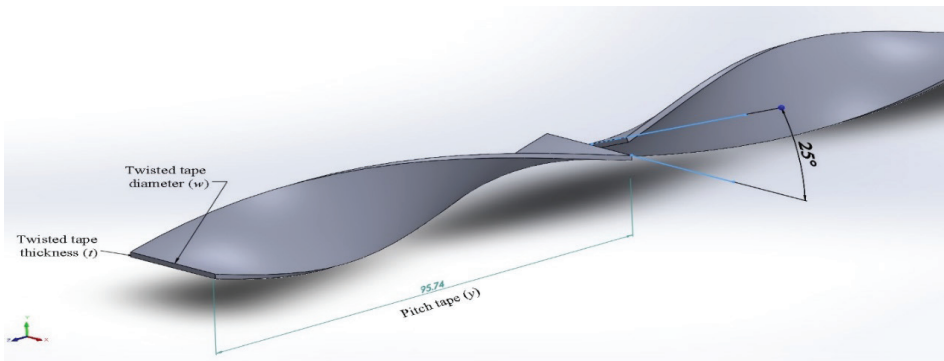
Figure 5 a. Twisted tape with 25 deg
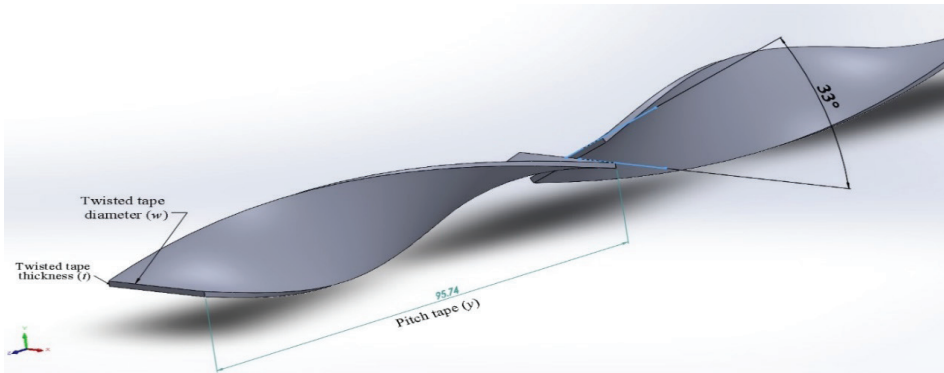
Figure 5 b. Twisted tape with 33 deg
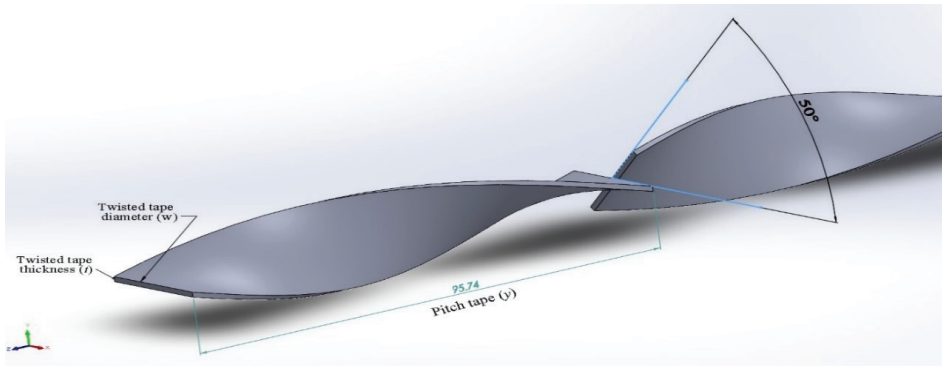
Figure 5 c. Twisted tape with 50 deg

3. SOLAR COLLECTOR PROCESSING

To collate the heat from sun rays, the rays fall on the upper tube surface and the reflector surface (PTC). The heat transfer in Figure 6 by several stages to reach the HTF. The heat transfer processes as a following: convection heat transfer between the HTF and absorber tube; conduction heat transfer in the absorber tube wall; radiation heat transfer from the absorber to the glass tube; conduction heat transfer in the glass tube; radiation heat transfer from the glass tube to the surrounding. The heat transfer from the glass tube to the surrounding is also occurred by convection and radiation, where the convection is may be forced or natural, relying on climate there is wind about the glass tube (Ananthsornaraj and Reddy 2015)
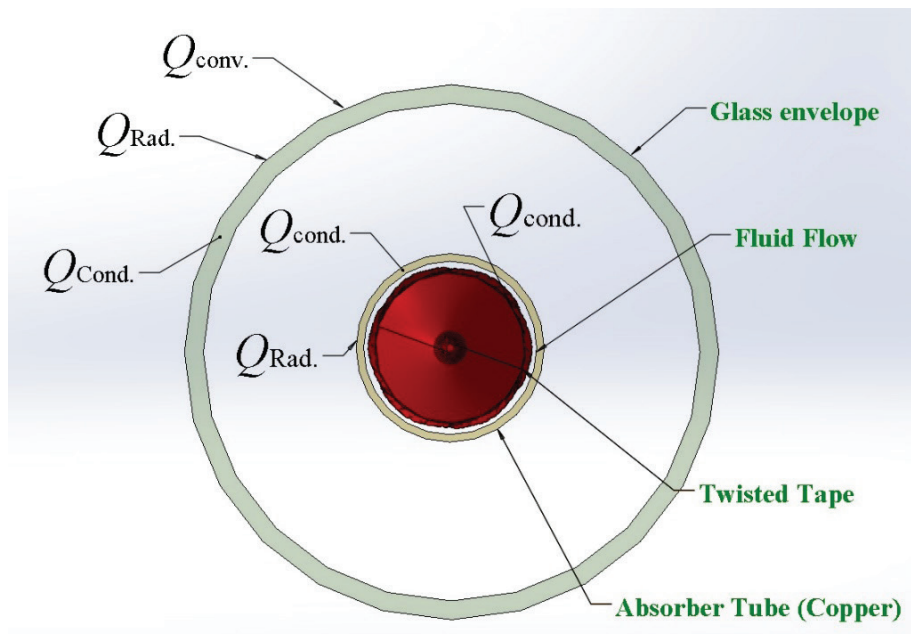
Figure 6. Heat transfers distribution on tubes

In the lower surface, the parabolic trough collector reflects rays to the lower side of the glass tube, but the amount of concentration heat is larger than the upper surface because the rays having concentrated and reflected by PTC so can neglect the heat energy which directly from the sun to upper surface in Figure 7.
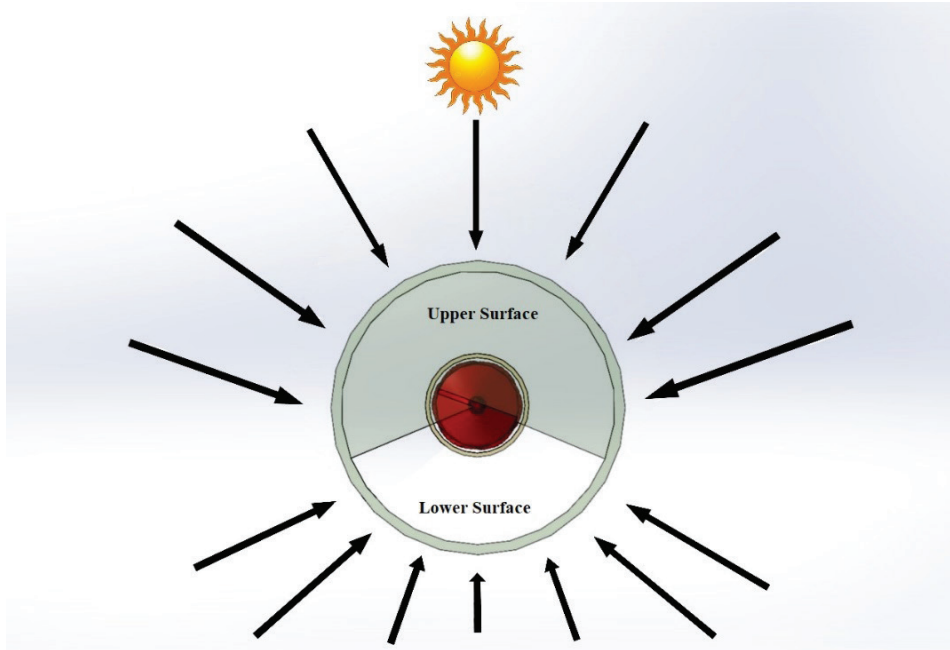
Figure 7. The upper surface and lower surface in the model

4. GOVERNING EQUATIONS

To estimate the thermal performance of PTC by the energy balance between the useful energy coming from the sun and heat transfer fluid HTF (Gianluca Coccia Giovanni Di Nicola Alejandro Hidalgo, n.d.). The thermal performance is steady-state condition and one dimensional, the heat transfer in the supporting bracket was neglected.

$$I_{abs} = Q_u + Q_{rad.abs} + Q_{conv.abs} \tag{4.1}$$

Where I_{abs} is the beam radiation reflected to absorber tube, Q_u is the useful heat will transfer to heat transfer fluid HTF, $Q_{rad.abs}$ is a heat loss from an absorber tube to glass envelope by radiation heat transfer, $Q_{conv.abs}$ is a heat loss from an absorber to a glass envelope by convection heat transfer(neglected). The beam radiation reflected to the absorber tube can calculate from in given equation:

$$I_{abs} = \rho \tau \alpha C I = \rho \tau \alpha C A_{ref} G \tag{4.2}$$

Where (C) concentrates ratio, (I) is solar energy that fell on the collector aperture area, and (G) is solar intensity (W/m²).

4.1 Heat Transfer in the Absorber Tube

Conduction heat transfer losses occur in absorber tube by using the equation :

$$Q_{cond.abs} = 2\,\pi\,L_{abs}\,k_{abs}\,\frac{(T_{abs.o} - T_{abs.i})}{\ln\left(D_{abs.o}/D_{abs.i}\right)} \tag{4.3}$$

where L_{abs} is the length of an absorber tube k_{abs} is a thermal conductivity of an absorber copper tube, $T_{abs.o}$ is outer the absorber temperature, $T_{bas.i}$ is inner of the absorber temperature, $D_{abs.o}$ is outer of the absorber diameter, $D_{abs.i}$ is inner the absorber diameter.

4.2 Heat Transfer in Absorber Tube to Glass Envelope

Thermal loss in an absorber tube occurs by radiation heat transfer only and convection heat transfer does not occur because of the vacuum between an absorber and a glass (Performance 2018).To evaluate radiation heat transfer in the equation:

$$Q_{rad.abs} = \sigma\varepsilon^{*}\pi D_{abs.o}\;L_{abs}(\,T_{abs.o}^{4} - T_{g.i}^{4}\,) \tag{4.4}$$

Where σ is Stefan-Boltzmann constant (5.67×10^{-8} W/m^2K^4), $T_{g.i}^{4}$ is inner glass temperature, ε^{*} for long concentric cylinder is:

$$\varepsilon^{*} = \left[\frac{1}{\varepsilon_{abs}} + \frac{1-\varepsilon_{g}}{\varepsilon_{g}}\left(\frac{D_{abs.o}}{D_{g.i}}\right)\right]^{-1} \tag{4.5}$$

The ε_{abs} is the emissivity for absorber tube and ε_{g} for glass envelope, $D_{g.i}$ inner diameter for a glass envelope.

4.3 Heat Transfer in the Glass Envelope

In glass envelope also will occur conduction heat transfer losses like in absorber tube by using the equation:

$$Q_{cond.g} = 2\,\pi\,L_{g}\,k_{g}\,\frac{(T_{g.i} - T_{g.o})}{\ln(D_{g.o}/D_{g.i})} \tag{4.6}$$

Where L_{g} is a length for glass envelope, k_{g} thermal conductivity for a glass, $T_{g.i}$ inner temperature for glass, $T_{g.o}$ outer temperature for glass, $D_{g.o}$ outer diameter for glass envelope.

4.4 Heat Transfer in the Glass Envelope to Ambient

The outer surface for glass envelope there is two types for heat transfer losses, first the radiation heat transfer between outer surface for glass and sky as given in the equation:

$$Q_{rad.g} = \sigma \, \varepsilon_g \, \pi \, D_{g.o} \, L_g \left(T_{g.o}^4 - T_{sky}^4\right) \tag{4.7}$$

The second is external convection heat transfer for the equation :

$$Q_{conv.g} = h_{air} \pi \, D_{g.o} L_g \left(T_{g.o} - T_{air}\right) \tag{4.8}$$

Where T_{air} is ambient temperature, h_{air} is a heat transfer coefficient for air can be defined in the equation:

$$h_{air} = \frac{Nu_{air} \, k_{air}}{D_{g.o}} \tag{4.9}$$

Where Nu_{air} is Nusselt number for air, k_{air} thermal conductivity for air can be calculated from film temperature (Gianluca Coccia Giovanni Di Nicola Alejandro Hidalgo, n.d.) :

$$T_{film} = (T_{g.o} + T_{air})/2 \tag{4.10}$$

The Nu_{air} is dependent on the wind outer surface for glass envelope if there is any wind that is main forced convection heat transfer defined from Churchill and Bernstein equation (CENGEL 2011):

$$Nu_{air} = 0.3 + \frac{0.62 \, Re_{air}^{1/2} \, Pr^{1/3}}{\left[1 + \left(0.4/Pr\right)^{2/3}\right]^{1/4}} \left[1 + \left(\frac{Re_{air}}{282,000}\right)^{5/8}\right]^{4/5} \tag{4.11}$$

Re_{air} is Reynolds number for air at T_{film}, Pr is Prandtl number for air at T_{film}.

If the surrounding without wind is that main free convection heat transfer ($10^5 < Re_{air} < 10^{12}$) defined from long horizontal cylinder equation (Gianluca Coccia Giovanni Di Nicola Alejandro Hidalgo, n.d.) :

$$Nu_{air} = \left\{0.60 + \frac{0.387 \, Re_{air}^{1/6}}{\left[1 + \left(0.559/Pr_{air}\right)^{9/16}\right]^{8/27}}\right\}^2 \tag{4.12}$$

4.5 Heat Transfer in Absorber Tube to Heat Transfer Fluid

The useful heat will transfer from the inner surface absorber tube to heat transfer fluid HTF be internal convection heat transfer to calculated by utilizing the energy balance in fluid volume (Performance 2018) :

$$Q_u = \dot{m} \, c_p \left(T_{out} - T_{in}\right) \tag{4.13}$$

Where $\dot{m}$ is a mass flow rate for HTF, c_p is the specific heat capacity at constant pressure. to determine heat transfer to fluid in an equation :

$$Q_u = A_{abs.i}\, h_f \left(T_{abs.i} - T_{film}\right) \tag{4.14}$$

Where $A_{abs.i}$ is an area of inner surface for absorber tube, h_f is a heat transfer coefficient for HTF to evaluated by the equation:

$$h_f = \frac{Nu_f\, k_f}{D_{abs.i}} \tag{4.15}$$

Where Nu_f is the Nusselt number for fluid, k_f is the thermal conductivity for fluid. To find the Nusselt number for turbulent flow and smooth absorber ($Re > 2300$) from Dittus–Boelter correlation equation:

$$Nu_f = 0.023\, Re^{0.8}\, Pr^{0.4} \tag{4.16}$$

The Reynolds number Re and Prandtl number Pr can be defined in the following (Bellos and Tzivanidis 2018)(Performance 2018):

$$Re = \frac{4\,\dot{m}}{\pi\, D_{abs.i}\, \mu_f} = \frac{\rho_f\, v_f\, D_{abs.i}}{\mu_f} \tag{4.17}$$

$$Pr = \frac{\mu_f\, c_p}{k_f} \tag{4.18}$$

Where ρ_f is the density for fluid, v_f is the velocity for fluid, μ_f Dynamic viscosity for fluid.

4.6 Concentration Ratio

Is the ratio between reflector surface area to absorber tube area, calculate the concentrate ratio that incoming from solar beam radiation to the absorber tube in the equation :

$$C = \frac{A_{ref}}{A_{abs}} = \frac{W_{ref}\, L_{ref}}{\pi\, D_{abs.o} L_{abs}} \tag{4.19}$$

Where A_{ref} area of parabolic trough collector surface, A_{abs} area of the absorber tube.

4.7 Efficiency of Parabolic Trough Collector (PTC)

The efficiency of PTC η can evaluate from the useful heat Q_u to HTF and the solar energy Q_s that fell on a collector aperture area in an equation:

$$\eta = \frac{Q_u}{Q_s} = \frac{m\, c_p (T_o - T_i)}{A_{ref}\, G} \tag{4.20}$$

4.8 Continuity, Momentum, and Energy

For turbulent steady, incompressible flow, no-slip conditions, constant thermophysical properties for the working fluid, the governing equations (Mahmoud, Abbas, and Khudheyer 2020) can be illustrated as:

Mass conservation :

$$\frac{\partial(\rho u_i)}{\partial x_j} = 0 \tag{4.21}$$

Momentum equation :

$$\frac{\partial(\rho u_i u_j)}{\partial x_j} = -\frac{\partial P}{\partial x_i} + \frac{\partial}{\partial x_j}\left[\mu\left(\frac{\partial u_i}{\partial x_j} + \frac{\partial u_j}{\partial x_i}\right) + \left(-\rho\overline{u_i' u_j'}\right)\right] \tag{4.22}$$

Energy equation :

$$\frac{\partial}{\partial x_j}(\rho u_i T) = \frac{\partial}{\partial x_j}\left(\left(\mu\frac{\partial u_i}{\partial x_j} + \mu_t\frac{\partial u_j}{\partial x_i}\right)\frac{\partial T}{\partial x_j}\right) \tag{4.23}$$

Where ρ density, u velocity, u' fluctuated velocity, P pressure , T temperature , μ dynamic viscosity and μ_t turbulent dynamic viscosity.

5. NUMERICAL ANALYSIS

5.1 Design Modeling

ANSYS design modeler had been used to sketch the absorber tube with a twisted tape inserted, of 1220 mm length, and 71 mm outer diameter (glass envelope)(Bhakta, Panday, and Singh 2018), by using a sweep tool with a pitch of (95.74 mm). It can neglect the direct solar rays from the sun and depend only on the radiation solar energy from the parabolic mirror because of the concentration ratio $(C) \approx 20$, this is mean over 10 (Duffie et al. 2013), the other outer surface was limited by the used Face Split and Edge Split tools to divide the tube edges into two sides. Table 2 shows the boundary conditions values used in this numerical study on 15th September at 9:00 am.

Table 2. Boundary conditions for this study

Specifications	Inlet water temperature	Inlet fluid velocity	Concentrated rate on the lower surface	Direct normal solar energy on the upper surface	Turbulence intensity for: plain, 25°,33°, 45°,50°, 55°,60°
Boundary conditions	300 K	0.03 m/s	8817 w/m²	589 w/m²	10.36 , 11.85 , 13.54 , 11.45 , 14.5 , 11.85 , 12.77

5.2 Grid Generation and Mesh Independency

ANSYS software was used to mesh the domain. In this study, in this study structural mesh with Hexa element type was used, mesh generation cross-section in Figure 7, on a long pipe with twisted tape. Many grid sensitivities test in Table 3, to ensure that the results are grid-independent, and 3652389 cell number was selected for all the computations done in the present study that for outlet temperature and when the number of elements exceeds these amounts, no effect on the results can be obtained.

Table 3. Element numbers for different geometries verifying grid independence validation
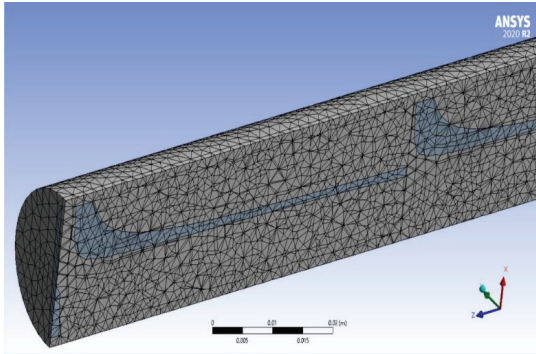
Figure 7. Effect of mesh generation on the tube and twisted tube

Test No.	Mesh	T_{out} (K)	Error %
1	96787	365.28	-
2	313928	361.1	1.1
3	1125926	359.88	0.3
4	2362626	358.64	0.3
5	3652389	358.3	0.09
6	3653675	358.3	0

5.3 Numerical Modeling and Analysis

This study utilized and created a mesh with three dimensional; heavy grids were created close to the bellows where a significant temperature difference occurs. The heat transfer issue was resolved by using the CFD software ANSYS FLUENT 2020R2. In advection terms in momentum and energy equation, a SIMPLE algorithm was utilized to couple the pressure and velocities using the second-order upwind procedure. Concentrated solar radiation flux was defined by utilizing User-Defined Functions (UDF) on the circumferential glass envelope and selective coating. All the equation was solved by used second order. For continuity, momentum, and energy equations the convergence standard was adjusted to 10^{-6}. The radiation of heat transfer loss from the absorber tube count on the emissivity, temperature, and surrounding object's temperature of the tube. A surface-to-surface simulated radiation model was used to supposed the absorber tube and the glass envelope were to be gray and diffuse (Ananthsornaraj and Reddy 2015).

6. RESULTS AND DISCUSSIONS

The performances change numerically on the tube with 4.787 twist ratio and without twisted tape (plain) by using water at working fluid, the solar intensity recorded in Istanbul- Turkey with latitude 41° N and longitude 28.97° E, for 4 recommended months (Duffie et al. 2013) on 15th September,15th October, 14th November, and 10th December from 9:00 am to 3:00 pm.

6.1 Model Validation

6.1.1 Validation with correlations of Eiamasa-ard et al. (Eiamsa-ard, Thianpong, and Eiamsa-ard 2010)**:**

To validating the results of this study, the tube with and without twisted tape is compared to (Eiamsa-ard, Thianpong, and Eiamsa-ard 2010) correlations for the results are shown in Figure 8. The comparison shows accepted with 3% and 5% variation of Nusselt number for tube with and without twisted tape, respectively.
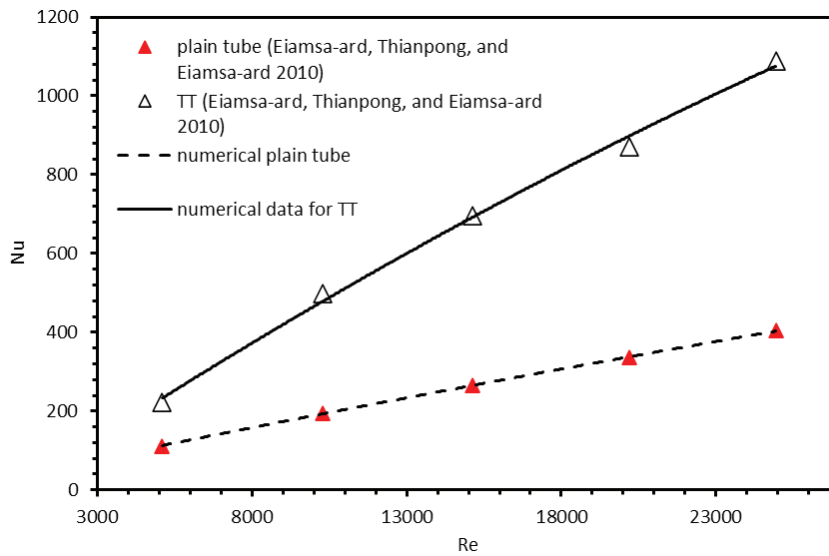
Figure 8. Relation between Nusselt number and Reynolds number

6.1.2 Code validation with Amit K. Bhakta et al.(Bhakta, Panday, and Singh 2018) **:**

The solar intensity measured experimental in India with latitude 23.47° N and longitude 86.30° E on 30th April from 9:00 am to 3:00 pm in Figure 9, are compared with numerical study results by using ANSYS FLUENT 2020 R2 software to found it.
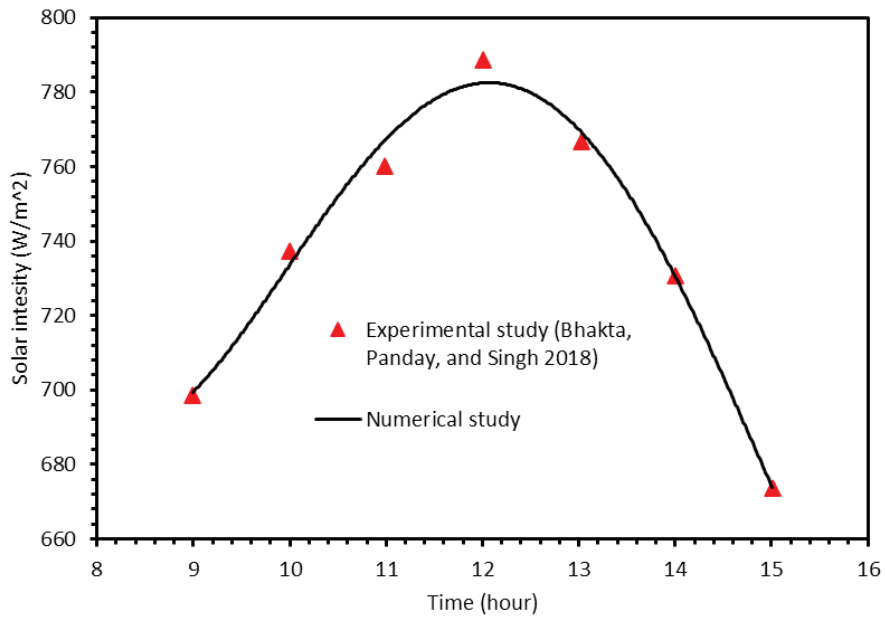
Figure 9. Variation of solar intensity with time for the experimental and numerical study

In Figure 10 outlet water temperature recorded experimental in India compared with the numerical result in same physical parameter and conditions at same day and time.
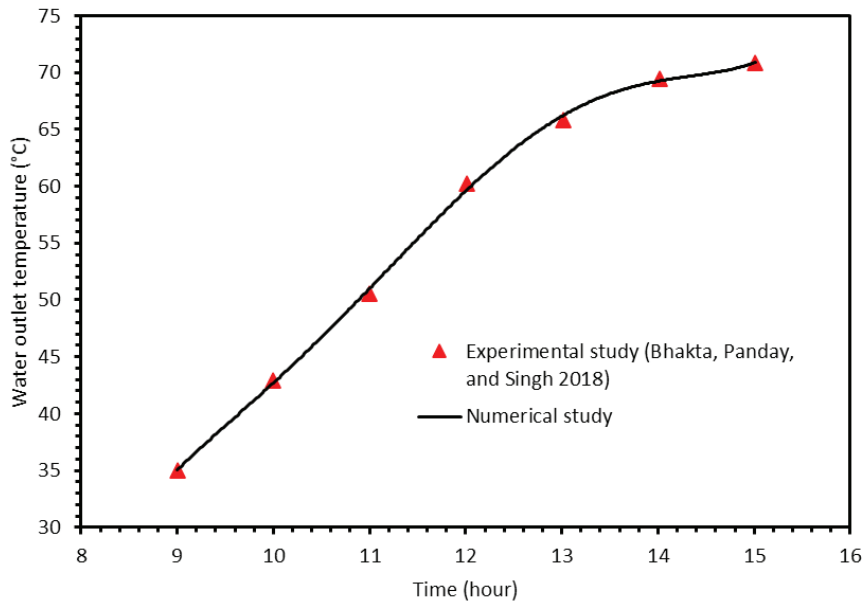
Figure 10. The variation of outlet water temperature with time

The thermal efficiency shown in Figure 11 with time for 4.747 twisted tape ratio which increases from 9:00 am to noon and after that decreases until to 3:00 pm, experimentally, and numerical results in tube insert (TT), the peak value at noon because in this time the solar intensity maximum value.
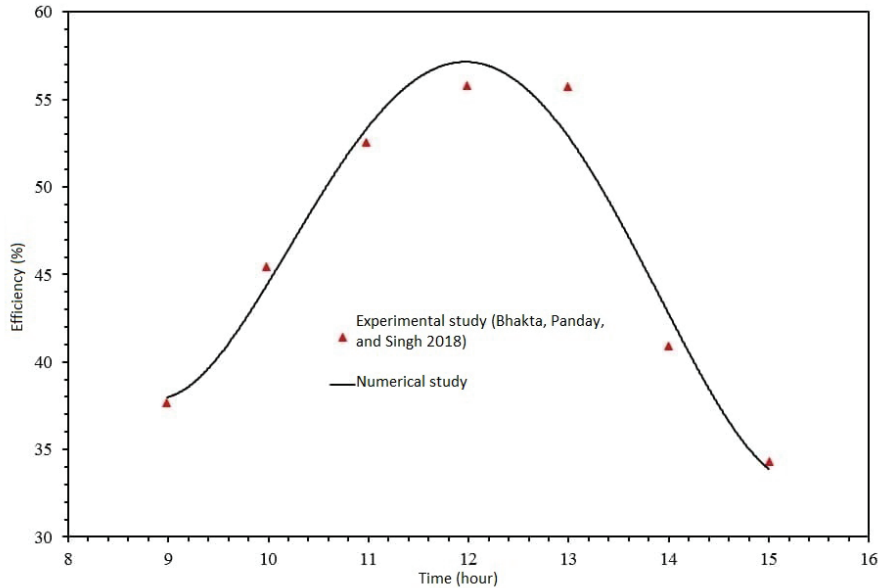
Figure 11. Validation of thermal efficiency with time

6.2 Outlet Temperature

The fluid inters to the tube without twisted tape (plain tube) in Figure 12 and slowly starts heating at first from the lower surface side of the tube to fluid due to the concentrated heat transfer from the reflector, the water temperature does not effectively well in the center of the tube with the heat comes from the collector because of there is not any method to enhance heat transfer like a passive or active. In twisted tape with 25 deg. in Figure 13 the center of the tube heat slowly due to the twisted tape because strong turbulence led to swirl motion and made mixing between the water close to the surface and with the center tube. Twisted tape with 33 deg. in Figure 14 the water temperature in the center of the tube is greater than the twisted tape with 25deg due to the increased obstruction of the water by increasing the angle degree and that is means increasing heat transfer coefficient. Figure 15 shows twisted tape with 50 deg. , the outer surface temperature reached to 432 k and the water temperature in the center of the tube reaches about 350 k and this temperature is more than other twisted tube angles.
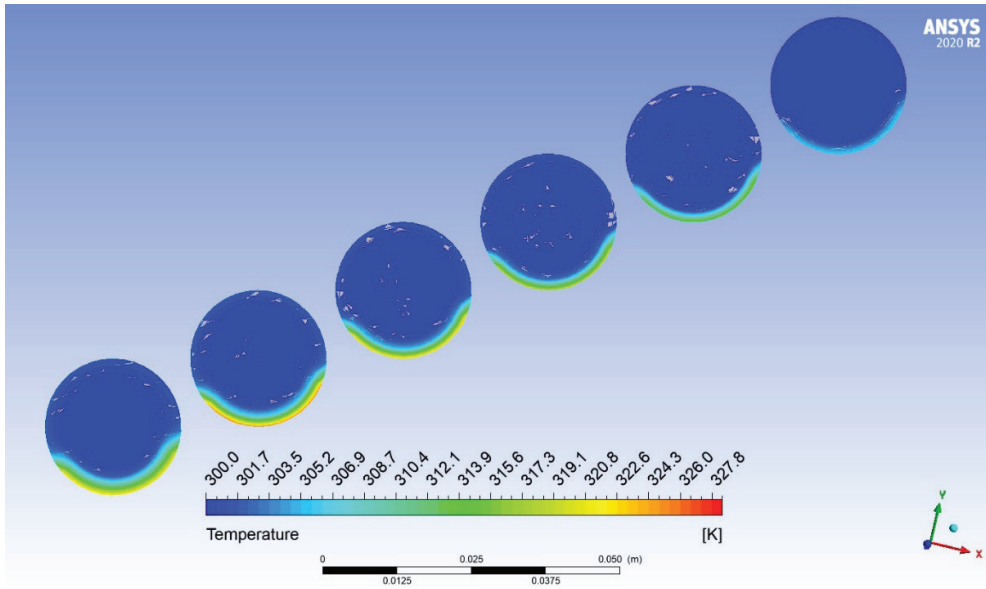
Figure 12. Temperature distribution inside the plain tube
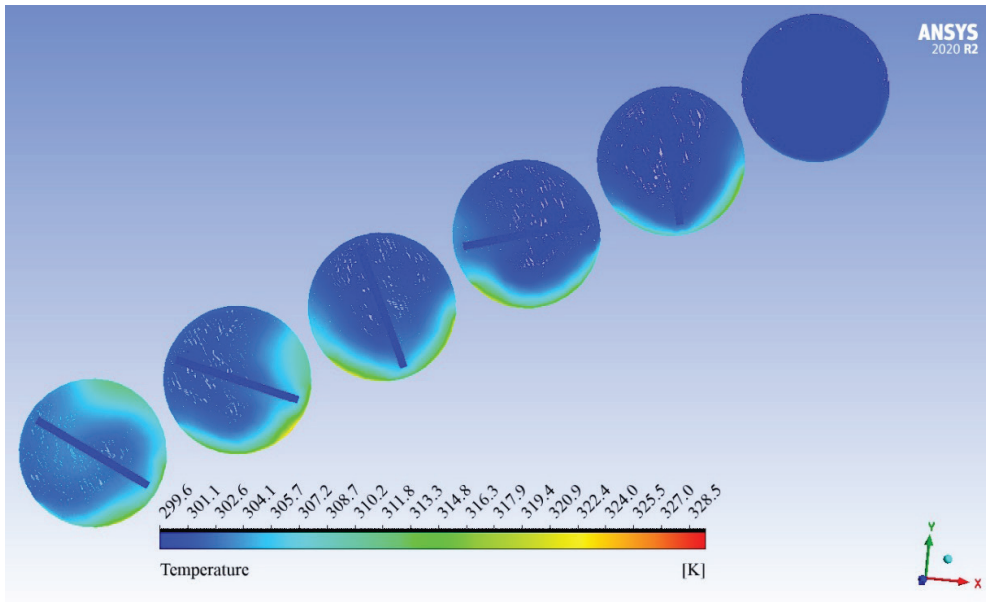
Figure 13. Temperature distribution inside twisted tape with 25 deg
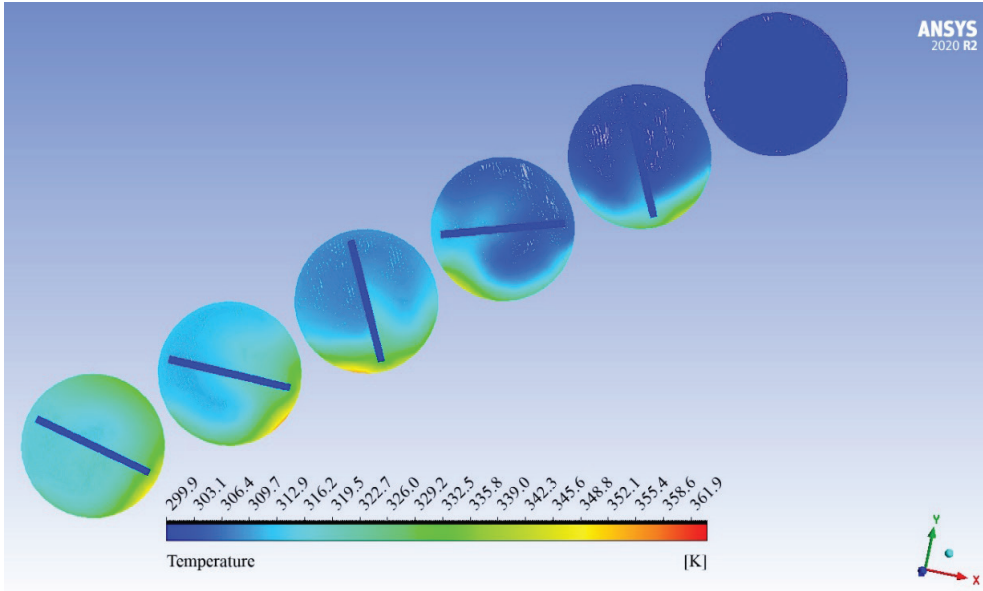
Figure 14. Temperature distribution inside twisted tape with 33 deg
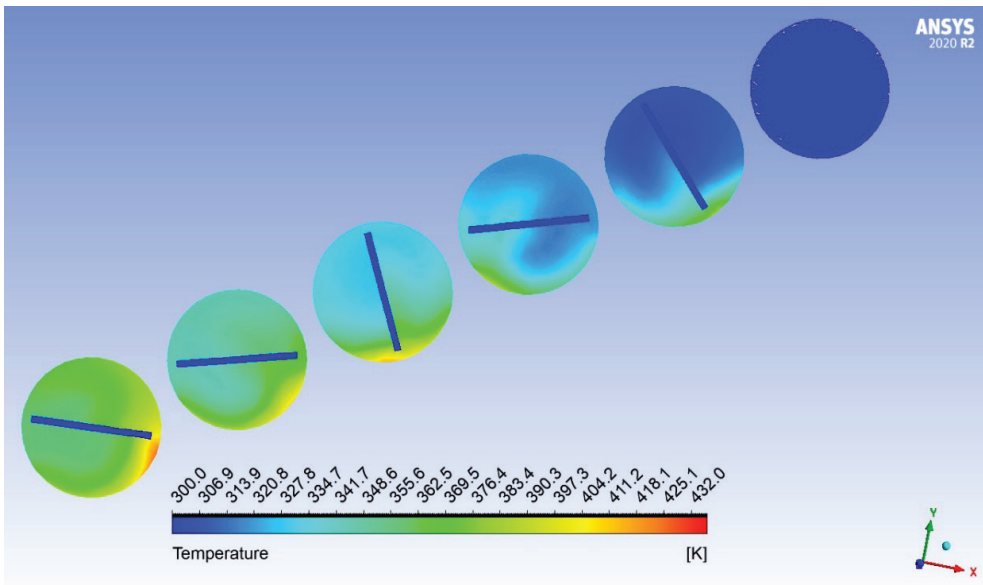
Figure 15 Temperature distribution inside twisted tape with 50 deg

The numerical result in Figure 16 recorded on 15th September in Istanbul the twisted tape with 50 deg. was recorded at a greater outlet temperature of 69.84 °C, twisted tape with 25°, 33°, 45°, 50°, 55°, and 60°. were recorded 59.87 °C, 64.84 °C, 68.81 °C, 69.84 °C, 57.49 °C, and 62.87 °C respectively. plain tube recorded 55.18 °C. Found increasing in outlet temperature of 7.83%, 14.89%, 19.57%, 21%, 4.76%, and 12.23% for twisted tape with 25°, 30°, 45°, 50°, 55°, and 60° respectively, compared with the plain tube.
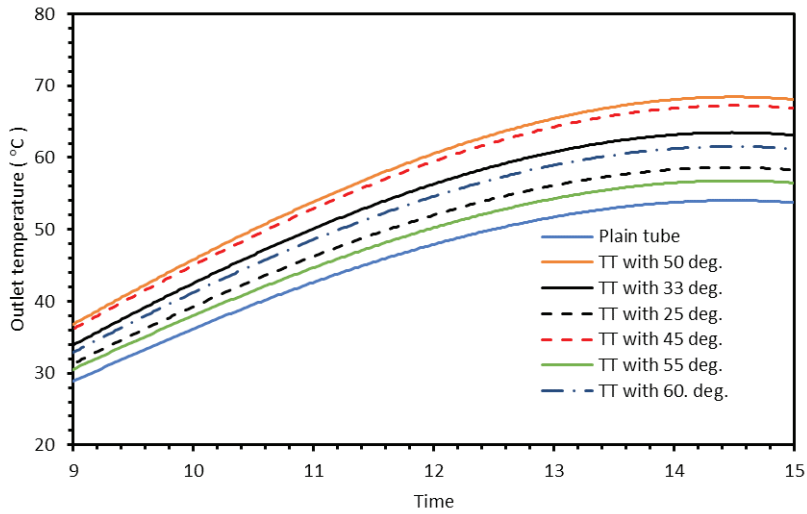
Figure 16. Water outlet temperate changes with time

6.3 Surface Temperature

The surface temperature was made different effect in Figure 5.11 when changing the twisted tape angles on 15th September, twisted tape with 50 deg. was recorded greater surface temperature. Found increasing in surface temperature of 9.4% , 16.34% , 20.92% , 24.61% , 6.37% , 13.71% for twisted tape with 25°, 33°, 45°, 50°, 55°, and 60° respectively, compared with the plain tube. The four recommend months (15th September, 15th October, 14th November, and 10th December) (Duffie et al. 2013) in Figure 17 discusses using twisted tape with 50 deg. the 15th of September recorded the best month because the solar intensity was greater than the other months, that is means will get more useful heat gain and more efficiency.
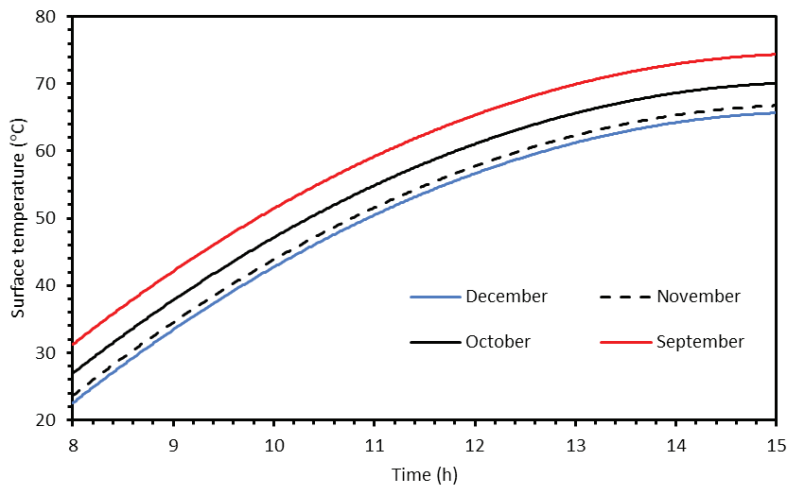
Figure 17. Changes surface temperature for 4 months with time

6.4 Heat Transfer Characteristics

The effect of twisted tap angles on Nusselt number (Nu) with different Reynolds number on 15th September in Figure 18 shows Nusselt number increase with increasing Reynolds number due to turbulent flow that was generated by twisted tape, therefore, created swirl flow and made mixing between water closer in surface and with the water in the center of the tube. Nusselt number increases by 18.51% , 39.88% , 41.01% , 43.95% , 12.38% , and 22.4% for twisted tape with 25°, 33°, 45°, 50°, 55°, and 60° respectively, compared with the plain tube.
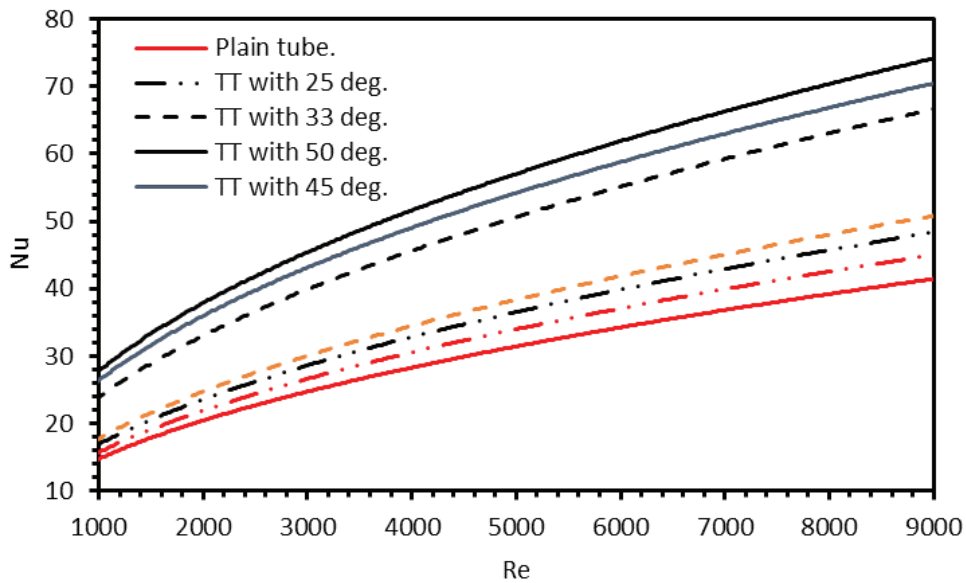
Figure 18. (Nu) validation with (Re) for 6 different angles and plain tube

6.5 Fraction Factor

The fraction factor decreases when increasing the Reynolds number in Figure 19, the surface area of twisted tape with 50 deg. was larger than other twisted taped angles and plain tube, which is a mean increase in disturbance according to swirl flow that was generated by the twisted tape (Yaningsih and Wijayanta 2018). Twisted tape with 25°, 33°, 45°, 50°, 55°, and 60°. obtain 38.66%, 52.08%, 60.51%, 71.77%, 67.60%, 69.73% respectively compared with the plain tube.
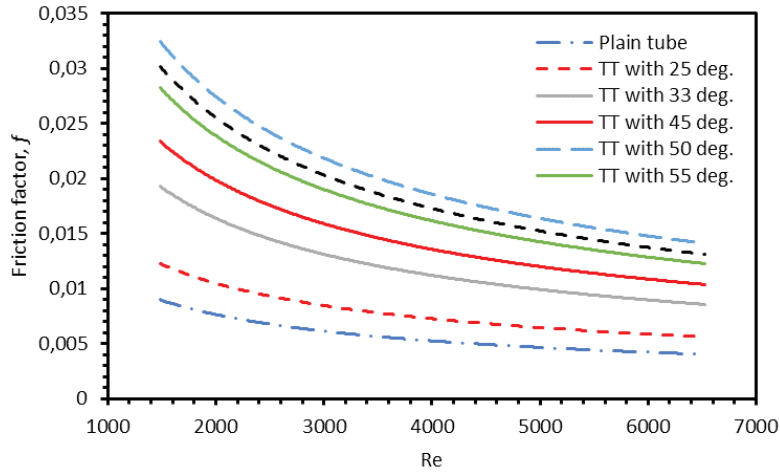
Figure 19. Change of friction factor with Reynolds number

6.6 Thermal Performance Factor

The thermal performance factor with Reynolds number in Figure 20 explains three different twisted tape angles and plain tube. The thermal performance factor decreasing when increasing the Reynolds number, This indicates that twisted tape cause to creates turbulently and swirl flow to enhance heat transfer in the tube (Zhang et al. 2019). The thermal performance factor gave advanced results in 6 different twisted tape angles according to the plain tube, in a range between 0.8899 to 1.1212, 0.9022 to 1.1900 , 0.9533 to 1.2324 , 0.9930 to 1.2838 , 0.8187 to 1.0315 and 0.8300 to 1.0948 , for twisted tape with 25°, 33°, 45°, 50°, 55°, and 60° respectively. 0.7123 to 0.8974 for plain tube.
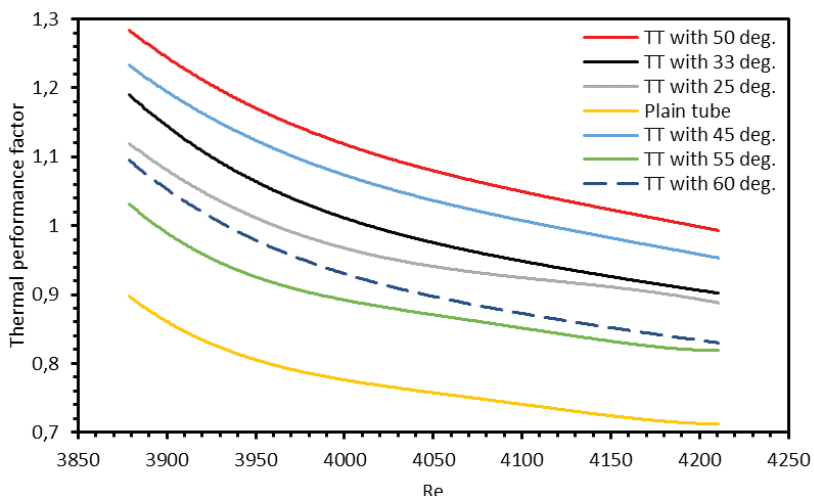
Figure 20. Relation between thermal performance factor and Re

7. CONCLUSION AND RECOMMENDATIONS

7.1 Conclusion

In this current study, the useful heat gain comes from solar intensity falling on the parabolic solar collector reflected to the absorber tube with twisted tape insert (made from aluminum), with six different angles (25°, 33°, 45°, 50°, 55°, and 60°). This enhanced the heat transfer, Nusselt number, and friction factor, because of increased surface area, and due to turbulent and swirling motion. It found that outlet temperature rising by 7.83%, 14.89%, 19.57%, 21%, 4.76%, and 12.23% for twisted tape with 25°, 33°, 45°, 50°, 55°, and 60° respectively, compared with the plain tube. The thermal performance factor gave advanced results in 6 different twisted tape angles compared with the plain tube, the best one at the twisted tape with 50 deg. In a range between 0.8899 to 1.1212, 0.9022 to 1.1900 , 0.9533 to 1.2324 , 0.9930 to 1.2838 , 0.8187 to 1.0315 and 0.8300 to 1.0948 , for twisted tape 25°, 33°, 45°, 50°, 55°, and 60° respectively. 0.7123 to 0.8974 for plain tube.

7.2 Recommendations for Future Works

• Effect of nanofluids on the thermal performance of solar parabolic collector.

• An empirical correlation for thermal efficiency of the solar parabolic collector with different positions in Turkey.

• Thermal performance enhancement for the solar parabolic collector with triple twisted tape insert.

8. REFERENCES

Ananthsornaraj, C., and K.S. Reddy. 2015. Numerical Investigation of Solar Parabolic Trough Receiver under Non Uniform Solar Flux Distribution. ISES Solar World Congress 2015, Conference Proceedings, no. November: 620–32. https://doi.org/10.18086/swc.2015.04.08.

Bellos, E., and C. Tzivanidis. 2018. Assessment of the Thermal Enhancement Methods in Parabolic Trough Collectors. International Journal of Energy and Environmental Engineering 9 (1): 59–70. https://doi.org/10.1007/s40095-017-0255-3.

Bellos E., and C. Tzivanidis. 2018. Analytical Expression of Parabolic Trough Solar Collector Performance."https://doi.org/10.3390/designs2010009

Bhakta, A.K., N.K. Panday, and S.N. Singh. 2018. Performance Study of a Cylindrical Parabolic Concentrating Solar Water Heater with Nail Type Twisted Tape Inserts in the Copper Absorber Tube. Energies 11 (1): 1–15. https://doi.org/10.3390/en11010204.

Cengel, Y.A. 2011. HEAT TRANSFER SECOND EDITION A Practical Approach. MacGraw-Hill. https://doi.org/10.1007/978-3-642-20279-7_5.

Duffie, J.A., W.A. Beckman, S.B. Prasad, J.S. Saini, K.M. Singh, S. Thakur, N.S. Thakur, R. Karwa, and V. Srivastava. 2013. Wiley: Solar Engineering of Thermal Processes, 4th Edition - John A. Duffie, William A. Beckman. Energy Sources, Part A: Recovery, Utilization and Environmental Effects. Vol. 2013. https://doi.org/10.1080/15567036.2020.1764672%0Ahttp://dx.doi.org/10.1016/j.solener.2008.11.011%0Ahttp://eu.wiley.com/WileyCDA/WileyTitle/productCd-0470873663.html.

Eiamsa-ard, S., C. Thianpong, and P. Eiamsa-ard. 2010. Turbulent Heat Transfer Enhancement by Counter/Co-Swirling Flow in a Tube Fitted with Twin Twisted Tapes. Experimental Thermal and Fluid Science 34 (1): 53–62. https://doi.org/10.1016/j.expthermflusci.2009.09.002.

Ghadirijafarbeigloo, S., A.H. Zamzamian, and M. Yaghoubi. 2014. 3-D Numerical Simulation of Heat Transfer and Turbulent Flow in a Receiver Tube of Solar Parabolic Trough Concentrator with Louvered Twisted-Tape Inserts."Energy Procedia 49: 373–80. https://doi.org/10.1016/j.egypro.2014.03.040.

He, W., D. Toghraie, A. Lot, F. Pourfattah, and A. Karimipour. 2020. Effect of Twisted-Tape Inserts and Nanofluid on flow field and Heat Transfer Characteristics in a Tube. 110 (December 2019). https://doi.org/10.1016/j.icheatmasstransfer.2019.104440.

Hidalgo, G.C.G.N.A. n.d. 2016. Parabolic Trough Collector Prototypes for Low-Temperature Process Heat. SpringerBriefs in Applied Sciences and Technology 2016.

Khoshvaght-Aliabadi, M., and A. Feizabadi. 2020. Performance Intensification of Tubular Heat Exchangers Using Compound Twisted-Tape and Twisted-Tube. Chemical Engineering and Processing - Process Intensification 148 (December 2019): 107799. https://doi.org/10.1016/j.cep.2019.107799.

Mahmoud, M.S., A.S. Abbas, and A.F. Khudheyer. 2020. Solar Parabolic Trough Collector Tube Heat Transfer Analysis with Internal Conical Pin Fins. Journal of Green Engineering 10 (10): 7422–36.

Padilla, R.V. 2011. "Simplified Methodology for Designing Parabolic Trough Solar Power Plants."

Saravanan, A., J.S. Senthilkumaar, S. Jaisankar, and J. Ananth. 2019. Influence of Helix Twisted Tape on Heat Transfer and Friction Factor in Forced Circulation V-Trough Solar Water Heater. International Journal of Sustainable Energy 38 (2): 163–76. https://doi.org/10.1080/14786451.2018.1476352.

Sharma, K., and L. Kundan. 2014. Nanofluid Based Concentrating Parabolic Solar Collector. International Journal of Research in Mechanical Engineering and Technology 4 (October): 146–52.

Sivakumar, K., K. Rajan, T. Mohankumar, and P. Naveenchnadran. 2020. Analysis of Heat Transfer Characteristics with Triangular Cut Twisted Tape (TCTT) and Circular Cut Twisted Tape (CCTT) Inserts. In Materials Today: Proceedings, 22:375–82. Elsevier Ltd. https://doi.org/10.1016/j.matpr.2019.07.212.

Velazquez-lucho, K.M., and M. Robles. 2016. Parabolic Trough Solar Collector for Low Enthalpy Processes : An Analysis of the efficiency Enhancement by Using Twisted Tape Inserts. 93: 125–41. https://doi.org/10.1016/j.renene.2016.02.046.

Yaningsih, I., and A.T. Wijayanta. 2018. Concentric Tube Heat Exchanger Installed by Twisted Tapes Using Various Wings with Alternate Axes Concentric Tube Heat Exchanger Installed by Twisted Tapes Using Various Wings with Alternate Axes. 030005 (January 2017). https://doi.org/10.1063/1.4968258.

Zhang, S., L. Lu, C. Dong, S. Hyun. 2019. Thermal Characteristics of Perforated Self-Rotating Twisted Tapes in a Double-Pipe Heat Exchanger. Applied Thermal Engineering 162 (May): 114296. https://doi.org/10.1016/j.applthermaleng.2019.114296.